

Measuring Receptor/Ligand Interaction at the Single-Bond Level: Experimental and Interpretative Issues

CHENG ZHU,^{1,2} MIAN LONG,^{1,3,4} SCOTT E. CHESLA,^{1,5} and PIERRE BONGRAND⁶

¹Woodruff School of Mechanical Engineering and ²Coulter Department of Biomedical Engineering, Georgia Institute of Technology, Atlanta, GA; ³College of Bioengineering, Chongqing University, Chongqing 400044 and ⁴National Microgravity Laboratory, Institute of Mechanics, Chinese Academy of Science, Beijing 100080, People's Republic of China; ⁵Immucor, Inc., Norcross, GA; and ⁶INSERM U 387, Laboratoire d'Immunologie, Hopital de Sainte-Marguerite, BP 29, 13274 Marseille Cedex 09, France

(Received 19 June 2001; accepted 8 January 2002)

Abstract—There is increased interest in measuring kinetic rates, lifetimes, and rupture forces of single receptor/ligand bonds. Valuable insights have been obtained from previous experiments attempting such measurements. However, it remains difficult to know with sufficient certainty that single bonds were indeed measured. Using exemplifying data, evidence supporting single-bond observation is examined and caveats in the experimental design and data interpretation are identified. Critical issues preventing definitive proof and disproof of single-bond observation include complex binding schemes, multimeric interactions, clustering, and heterogeneous surfaces. It is concluded that no single criterion is sufficient to ensure that single bonds are actually observed. However, a cumulative body of evidence may provide reasonable confidence. © 2002 Biomedical Engineering Society.
[DOI: 10.1114/1.1467923]

Keywords—Sensitive force techniques, Probabilistic model, Adhesion likelihood, Attachment lifetime, Rupture force.

INTRODUCTION

The ability to measure molecular interactions at the single-bond level symbolizes a long-standing theoretical appeal, as it is thought to provide fundamental understanding of adhesive receptor/ligand binding. It can also offer insights to, and a basis for, modeling cellular adhesion mediated by multimolecular interactions. To experimentalists, measuring single-bond properties represents quite a technical challenge; yet such data may be easier to interpret, as the interaction has been reduced to its simplest form. In the past decade, there have been many experimental reports on attempts to observe the mechanical and chemical interactions of single ligand/receptor bonds. These experiments consisted of making a contact between two surfaces, respectively coated with low densities (or low affinity) of receptors and ligands to

produce rare adhesions, then monitoring their separation by forces ranging from several to several hundreds of piconewtons. The forces were generated by different procedures, including shear flow,^{2,22,43} biomembrane force probe,^{14,16,30} micropipette aspiration technique,^{38,39} atomic force microscope (AFM),^{17,26} optical tweezers,^{31,44} or microcantilever.⁴² The measured parameters included the likelihood of forming attachments at a given contact time,¹¹ the lifetime of attachments at a given force,² or the rupture force of attachments at a given rate of steadily increasing force.³⁰ While valuable information has been obtained from these experiments, it remains difficult to know with sufficient certainty that these measurements indeed probe single bonds, contrary to what was claimed by some. Not knowing what are actually measured obscures the interpretation of data and parameters derived from the data: Are these truly intrinsic properties of single bonds or apparent properties of multibond clusters?

In this commentary, using typical data generated from our laboratory, we examine evidence that has been used to support single-bond conditions in the literature. Specifically, we will consider the validity and caveats of the following points:

- (i) discontinuous and stochastic features;
- (ii) infrequency of binding events and their probabilistic analysis and Monte Carlo simulation;
- (iii) dissociation time course and first-order kinetics;
- (iv) quantal behavior;
- (v) multimeric interaction, clustering, and heterogeneous surface;
- (vi) rupture force and expected single-bond strength; and
- (vii) effects of sensitivity cutoff.

DISCONTINUOUS AND STOCHASTIC FEATURES

Why is it by no means obvious that single bonds are actually observed? Typical sizes of adhesion receptors

Address correspondence to Dr. Cheng Zhu, George W. Woodruff School of Mechanical Engineering and Wallace H. Coulter Department of Biomedical Engineering, Georgia Institute of Technology, Atlanta, GA 30332-0363. Electronic mail: cheng.zhu@me.gatech.edu

are of the order of 10 nm. At present no experimental technique exists that allows for direct visualization of single-bond events in real time. Therefore, the single-bond contention has to be inferred from analyses of the characteristics of what can be measured. It is thus useful to examine the previously used or potential new arguments that are considered as suggestive of single-bond events. What, then, are expected characteristics if the measurements reflect single-bond events?

The initial indication that what are being measured may be single-bond events is usually their discontinuous behavior. For example, titration of the surface density of P-selectin coated on a flow chamber floor led to a regime in which continuous rolling adhesion of leukocytes became no longer possible. Instead, flowing cells were observed to attach to and detach from the surface with abrupt changes in velocity.² Adhesions mediated by biotin/avidin or /streptavidin interactions were sometimes seen to rupture at discrete steps, as revealed by AFM measurements.¹⁷ Low density of E-selectin coated on the red blood cell (RBC) surface resulted in “point attachments” to the ligand-expressing cell that dissociated sequentially instead of “area attachments” that peeled off continuously, despite the fact that the two cells had been impinged onto each other by micropipette manipulation.²⁸

As the experimental conditions were progressively changed towards those under which adhesion was less and less favored (e.g., by diluting the site densities of the interacting molecules, reducing the time or area of their contact, or lowering their binding affinity), not only did binding events become discontinuous but they also appeared stochastic. The observed randomness seemed to be inherent to the interaction in question instead of being associated with experimental errors, as it became more significant when binding was less frequent but it was not reduced by increase in measurement accuracy. The appearance of behavioral discontinuity and randomness is strongly suggestive that these adhesions were mediated by a few bonds.¹² It seems logical to reason that the progression of such discontinuous and random behavior, as the binding sites are further diluted, may lead to single-bond conditions. The question is: is it always the case? If so, how to prove it? If not, under what circumstances is it not? To answer these questions requires that the seemingly discontinuous and random measurements be successfully modeled, simulated, and described using properties of the molecules under conditions in which a small number of them are interacting. Three types of measurements are discussed below: the occurrence, lifetime, and rupture force of adhesion.

INFREQUENCY OF BINDING EVENTS AND THEIR PROBABILISTIC ANALYSIS AND MONTE CARLO SIMULATION

A commonly used strategy to achieve, and argument for observing, single-bond events is their infrequent occurrence. If these focal and discrete adhesion events are mediated by a few bonds, they ought to follow the laws of small numbers. This is illustrated in Fig. 1, which shows results of a micropipette experiment similar to that described in Ref. 28. Here, a single RBC coated with a low density of P-selectin (a few molecules per micron square) was allowed to make repeated contacts with a human promyelocytic leukemia cell (HL-60) expressing P-selectin glycoprotein ligand 1 (PSGL-1). When two cells were moved apart, adhesion, if present, was detected as the flexible RBC membrane was deflected by a force of a few piconewtons. It was observed that the infrequent binding occurred as discrete attachment points that were spatially isolated. The frequencies p_n ($n = 0, 1, 2, 3, \dots$) of observing n -point attachments were found to follow a Poisson distribution, $p_n = (\langle n \rangle^n / n!) \times \exp(-\langle n \rangle)$ [Fig. 1(A)]. The Poisson distribution depends on a single parameter, the average number of point attachments $\langle n \rangle$, which can be related to the probability of adhesion, $P_{a|0}$, by $P_{a|0} = \sum_1^\infty p_n = 1 - \exp(-\langle n \rangle)$ [Fig. 1(B)]. It is thus possible to express the probabilities of having no attachment (p_0) and attachments by 1, 2, 3, ..., points (p_1, p_2, p_3, \dots) in terms of $P_{a|0}$. As can be seen, most of the observed adhesions were mediated by single-point attachments at low $\langle n \rangle$ and $P_{a|0}$ values. Such an agreement suggests that these point attachments were formed independently of each other and with equal probability, thereby behaving as quantal binding units.

It seems reasonable to hypothesize that the observed point attachments were individual bonds. A supporting evidence for this hypothesis is our remarkable ability to describe the likelihood for the random occurrence of these isolated and infrequent adhesions using probabilistic models for small system kinetics, which are formulated as a set of master equations.^{11,12,29,53} The master equations take different forms depending on the scheme and mechanism of the reaction. Here, we use a simple form to illustrate the various points discussed in this paper:³⁵

$$\begin{aligned} \frac{dp_n}{dt} = & (n+1)k_r^{(n+1)}p_{n+1} - \left[(A_c m_r - n)(A_c m_l - n) \frac{k_f^{(n+1)}}{A_c} \right. \\ & \left. + nk_r^{(n)} \right] p_n + [A_c m_r - (n-1)][A_c m_l - (n-1)] \\ & \times \frac{k_f^{(n)}}{A_c} p_{n-1}, \end{aligned} \quad (1)$$

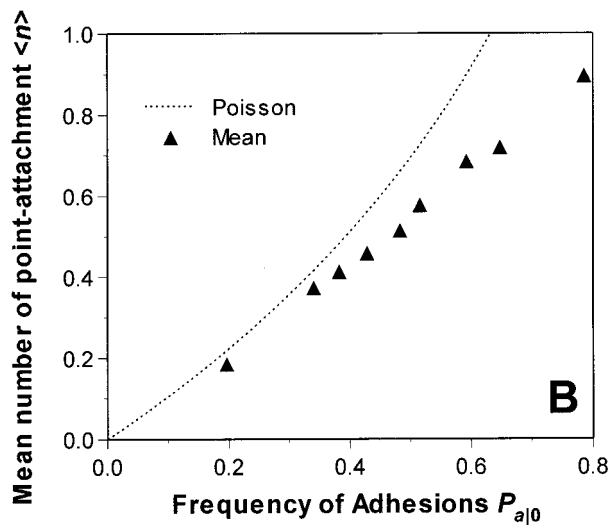
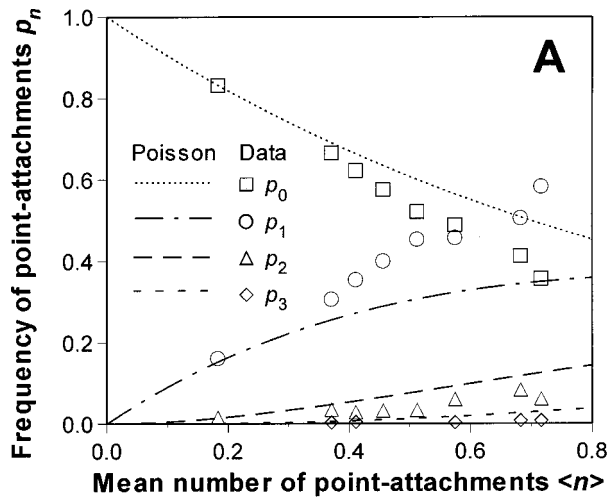


FIGURE 1. Comparison between measured (points) and predicted (curves) probabilities of having n ($= 0$ – 3) point attachments, p_n , as functions of the average number of point attachments, $\langle n \rangle$, (A) or $\langle n \rangle$ as a function of the probability of adhesion, $P_{a|0}$ (average over a narrow range within each bin), (B) for HL-60 PSGL-1 interacting with P-selectin coated on RBC. The predictions were calculated using the Poisson distribution (see the text). The experiment was done using the micropipette technique as described in Ref. 28. As $\langle n \rangle$ and $P_{a|0}$ increase, the higher p_1 and the lower p_2 and p_3 (A) and the lower $\langle n \rangle$ (B) experimental values than their Poisson counterparts may be due to observation errors. The determination of an adhesion to be a single-, double-, or triple-point attachment was made from a planar microscopic observation, which projected the circular contact disk onto a line. As such, the observation tended to overestimate p_1 and underestimate p_2 and p_3 , because multiple-point attachment might project as a single-point attachment from the sideview. This might also bias the calculations of mean and variance of the number of point attachments based on the measured p_n towards a lower $\langle n \rangle$ value, especially in high values of $\langle n \rangle$ and $P_{a|0}$, where multiple-point attachments are expected to be (and were observed to be) more frequent.

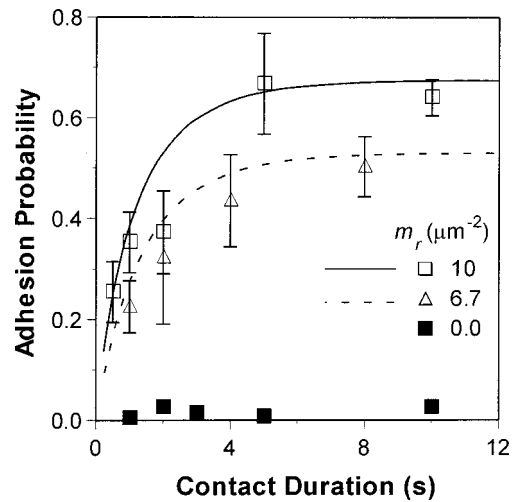


FIGURE 2. Kinetic analysis of adhesions mediated by a low number of bonds. Plotted are dependences on contact duration of probability of adhesion between PSGL-1 expressing HL-60 cells and RBC coated with different densities of P-selectin as indicated by different symbols. Data, measured with the micropipette, are presented as mean \pm SEM of 3–5 pairs of cells of 100 cycles each. Curves are theoretical fits to the data using a solution to Eq. (1) (see the text) with constant kinetic rates ($m_r A_c k_f^0 = 0.06 \mu\text{m}^2 \text{s}^{-1}$ and $k_r^0 = 0.55 \text{s}^{-1}$) after correction for the nonspecific adhesions (■) (Ref. 11).

where the same symbol p_n is used here to denote the probability of having n bonds. $k_f^{(n)}$ and $k_r^{(n)}$ are the respective forward- and reverse-rate coefficients for the formation and breakage of the n th bond, m_r and m_l are the respective densities of receptors and ligands, and A_c and t are the contact area and time.

An approximate analytical solution to Eq. (1) that satisfies the initial condition that there is no bond at $t = 0$ reads: $P_{a|0} = 1 - \exp\{-m_r m_l A_c K_a^0 [1 - \exp(-k_r^0 t)]\}$, where $K_a^0 \equiv k_f^0 / k_r^0$ is the binding affinity and the superscript 0 indicates that the binding parameters are evaluated at zero force and are assumed independent of n .¹¹ This model predicts the Poisson distribution seen in Fig. 1 and relates the average bond number to the molecular properties: $\langle n \rangle = m_r m_l A_c K_a^0 [1 - \exp(-k_r^0 t)]$. More importantly, it explains quite well the kinetics of the observed adhesion probability: $P_{a|0}$ increased with increasing contact time t initially and approached a steady state as t became large; and the $P_{a|0}$ vs t curves shifted upward as m_r or m_l increased (Fig. 2). By fitting the measured to predicted $P_{a|0}$ vs t curves in a range of m_r and m_l , one could determine the kinetic mechanism and derive the kinetic rate constants for the interacting receptors and ligands (Fig. 2, caption). The model has been tested extensively using two very dissimilar families of adhesion molecules (immunoglobulin superfamily and selectins) and similar members within each family (Fig. 2 and Refs. 10, 11, 28, and 49–51).

An alternative approach to treat the infrequent binding events is that of Monte Carlo simulations, which has been successfully used by several groups, primarily in modeling dynamic interactions of cells in a flow field.^{7,8,19,23–25,39,41,46} In this approach, the fate of a set of bonds is simulated to generate an ensemble of realizations for these random events from which various statistics are obtained, instead of solving the probabilities of having bonds in time from the master equations. Each simulation mimics an experimental measurement; thereby allowing for direct comparison between simulations and observations. For simple kinetic schemes, it can be readily shown that the stochastic criteria underlying the Monte Carlo simulation are equivalent to the kinetic laws on which the master equations are based.²⁷ Thus, the two approaches should provide the same results. However, for complex kinetic schemes, multimeric interactions, clustering, and heterogeneous surfaces, Monte Carlo simulations may be more easily implemented computationally because the stochastic criteria remain fairly simple at the level of individual molecules in elementary reaction steps. By comparison, inclusion of multiple levels of complexity likely results in complicated master equations that are no longer solvable analytically. Another computational advantage of the Monte Carlo approach is that simulations of chemical kinetics can be easily combined with simulations of other physical aspects, such as the motion of cells in a flow field. By comparison, solving the master equations simultaneously with equations governing other coupled mechanical processes can be challenging.

However, the successful modeling and simulation of the kinetic behavior of the observed point attachments by the kinetics of individual bonds does not prove that these point attachments are indeed single bonds. The reason for this, as pointed out by Piper *et al.*,³⁵ is that the same solution for p_n and $P_{a|0}$ will be obtained if n in Eq. (1) represents, instead of the number of bonds, the number of point attachments, each of which, in turn, consists of a cluster of m bonds. Although m_r and m_l in such a case should be interpreted as, instead of the densities of the receptors and ligands themselves, the respective densities of their clusters, this does not negate the ability for p_n to follow Poisson statistics and $P_{a|0}$ to fit the adhesion data. Only will the value and interpretation of the fitted parameter K_a^0 be different. Dilution of binding sites can reduce the average number and frequency of point attachments. However, this does not necessarily reduce the number of bonds per point attachment even if they are so diluted that, on average, most likely only one pair of molecules would be interacting. The reason is that dilute binding sites are not necessarily distributed uniformly. Clusters of binding sites may remain clustered no matter how dilute they are titrated, which will result in multi-

bond adhesions in spite of their discontinuity and infrequency.

DETACHMENT TIME COURSE AND FIRST-ORDER KINETICS

The second type of measured quantities is adhesion lifetimes, which is commonly performed using the flow chamber technique. Here, moving receptor-bearing cells tethered to the chamber floor coated with ligands of densities too low to support rolling. While the duration of any single arrest or tethering event seemed random, the histogram of a large number of these tether lifetimes revealed their underlying probability distribution, which should be governed by dissociation kinetics of the interacting molecules. If single bonds were essentially responsible for the observed tethering events, lifetimes of these events should follow single-bond kinetics. A commonly assumed form of this is first-order irreversible dissociation with an exponential distribution, $P_{a|1} = \exp(-k_r t)$, which is a simplest solution to Eq. (1), with all kinetic rates set to zero except $k_r^{(1)} (= k_r)$, $P_{a|1}$ is the probability for a cell to remain adherent at time t by a bond that initially exists at time 0. The subscript 1 is used to denote this initial condition $P_{a|1}(0) = 1$, allowing it to be distinguished from $P_{a|0}$, the probability for the presence of adhesion at time t under the initial condition $P_{a|0}(0) = 0$. Taking the natural log of the event frequency linearizes the lifetime histogram of first-order dissociation, and the slope of the line is equal to $-k_r$ (Fig. 3). Lifetime histograms that appear to be exponentially distributed have indeed been reported, and first-order irreversible dissociation kinetics has been widely used to analyze tether lifetimes mediated by selectin/ligand interactions measured in flow chamber experiments.^{1,2,9,33,36,37,40}

By comparison, if additional bonds are allowed to form after the cell has been tethered to the surface by the first bond, a nonlinear $\ln(P_{a|1})$ vs t curve will result (Fig. 3), given by $P_{a|1} = 1 - [1 - \exp(-k_r t)] \exp\{-m_r m_l A_c K_a [1 - \exp(-k_r t)]\}$.²⁷ To obtain this simple analytical solution all kinetic rates in Eq. (1) have been assumed independent of n (but nonzero), which tends to underestimate the curvature of the $\ln(P_{a|1})$ vs t curve. The hypothesis that applied force accelerates dissociation predicts that the larger the n , the smaller the $k_r^{(n)}$, because the force per bond is smaller. This leads to more bonds surviving a longer time. The nonlinearity is caused by the presence of multiple bonds and hence, the more bonds, the greater the curvature. Setting the cellular on-rate $m_r m_l A_c k_f$ to zero recovers the single-exponential distribution discussed earlier, as required.

Lowering the site density on the chamber floor may minimize the formation of multiple bonds by reducing the cellular on-rate, provided that the molecules are not

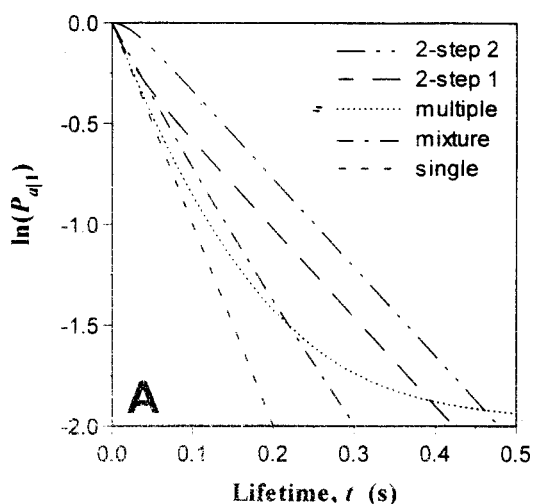
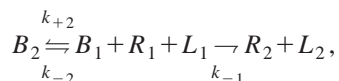


FIGURE 3. Comparison of indicated theoretical detachment curves. If governed by a single-step reaction, receptor-expressing cells tethered to the ligand-coated flow chamber floor by single bonds will follow first-order irreversible dissociation kinetics and display a straight line in the $\ln(P_{a|1})$ vs t plot (single), with the slope equal $-k_r$ ($=10 \text{ s}^{-1}$). By comparison, formation of additional bonds (with a cellular forward-rate $m, m, A_c, k_f^0 = 0.15 \text{ s}^{-1}$) after the initial tethering by the first bond results in a nonlinear detachment curve (multiple), although the initial slope of the curve near $t=0$ reports the correct k_r value. Single bonds of a two-step reaction scheme or dimeric bonds formed between dimeric molecules have double-exponential lifetime distributions that are concave or convex depending on whether the initial bond is metastable (or monomeric, two-step 1) or stable (or dimeric, two-step 2). So are two species of single bonds concurrently formed between two heterogeneous surfaces (mixture). For the kinetic rates chosen ($k_{-1} = 10 \text{ s}^{-1}, k_{-2} = k_{+2} = 20 \text{ s}^{-1}, k_{r1} = 10 \text{ s}^{-1}, k_{r2} = 5 \text{ s}^{-1}, \eta_1 = \eta_2 = 0.5$), the non-linearity is so mild that they appear as straight lines for the most part. Other parameters may give rise to highly curved detachment curves (Ref. 32).

clustered. For multimeric molecules such as P-selectin, dilution will result in lower density of multimers but may not reduce the number of molecules per multimer, as noted earlier.

The analysis of multimeric binding requires master equations that are more involved than Eq. (1). Perhaps the simplest multimeric binding case is that of dissociation of dimeric bonds, given by



where R , L , and B , respectively, denote receptor, ligand, and bond, with subscript 1 or 2 indicating monomeric or dimeric state, and k denote kinetic rates with subscript + and - indicating forward and reverse reaction, respectively. If the cell is bound by a B_1 bond at $t=0$ ($x=1$ case), the free arms of the dimeric receptor and ligand

(R_1 and L_1) may either bind to form a B_2 bond (which brings the cell to the $x=2$ case below) or the B_1 bond may dissociate, resulting in cell detachment from the surface. If the cell starts with a B_2 bond ($x=2$), either of its two arms may dissociate, bringing the cell to case 1. The probability for the cell to remain adherent at $t > 0$ is (B. Marshall and C. Zhu, unpublished results):

$$P_{a|x}(t) = \begin{cases} \left(1 - \frac{\lambda_2}{k_{-2}}\right) \frac{\lambda_1 e^{-\lambda_2 t}}{\lambda_1 - \lambda_2} - \left(1 - \frac{\lambda_1}{k_{-2}}\right) \frac{\lambda_2 e^{-\lambda_1 t}}{\lambda_1 - \lambda_2} & x=1 \\ \frac{\lambda_1 e^{-\lambda_2 t} - \lambda_2 e^{-\lambda_1 t}}{\lambda_1 - \lambda_2} & x=2 \end{cases}, \quad (2a)$$

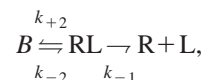
where

$$\lambda_{1,2} = \frac{1}{2}(k_{-1} + k_{-2} + k_{+2}) \pm \frac{1}{2}[(k_{-1} + k_{-2} + k_{+2})^2 - 4k_{-1}k_{-2}]^{1/2}. \quad (2b)$$

It is evident from Fig. 3 that the $\ln(P_{a|x})$ vs t curve is nonlinear: concave or convex depending on whether the cell is initially bound by a B_1 or B_2 bond.

However, dissociation curves of reactions other than first-order irreversible dissociation may not differ sufficiently from those expected for single bonds. This is illustrated in Fig. 3 by two dimeric dissociation curves calculated using Eq. (2). As can be seen, for the kinetic rates chosen, the curves appear as fairly straight lines for the most part. It is likely that the inherent errors in the flow chamber experiment will make it difficult to obtain lifetime measurements that detect the small curvatures seen in the initial portion of the theoretical curves. This is especially the case when both initial conditions are present, which is likely the case in real experiment, because the concave and convex curves compensate each other to give rise to an even more straight-line appearance. Thus, the apparent “good fit” of a straight line to the $\ln(P_a)$ vs t data is insufficient to ensure single bonds. An example that demonstrates this point will be discussed shortly.

Conversely, nonlinearity in the experimental $\ln(P_a)$ vs t curve is insufficient to rule out the possibility of single bonds. Single-bond interactions of complex reaction schemes may not obey first-order irreversible dissociation kinetics. Two examples are illustrated in Fig. 3. The first is a two-step binding, given by



where RL stands for a metastable receptor–ligand complex formed in the first step before forming a stable bond in the second step. Theoretical dissociation curves of this reaction are also given by Eq. (2), which can differ considerably from straight lines for certain kinetic rate values. Multistep single-bond binding was first suggested by Pierres *et al.*³² to explain the nonlinear appearance of their experimental $\ln(P_a)$ vs t curves obtained with the flow chamber.

Concurrent binding of multispecies of receptors and ligands between heterogeneous surfaces is another example that may result in nonlinearity in $\ln(P_a)$ vs t curves. This is also shown in Fig. 3 for comparison. In this example, the dual-species dissociation curve is given by $P_{a|1} = \eta_1 \exp(-k_{r1}t) + \eta_2 \exp(-k_{r2}t)$, where the non-negative η_i is the fraction of the i th species satisfying $\eta_1 + \eta_2 = 1$. Multispecies bindings may not be intended but often are inevitable in experiments. To study the molecules of interest they must be coated on the surface of the experimental system, such as the AFM tip, the flow chamber floor, beads, or RBC. Commonly used coating strategies, such as physisorption and biotin–streptavidin coupling, immobilize molecules with random orientations, thereby creating a heterogeneous binding surface. Even if molecules are uniformly immobilized, other undefined species may be involved, often manifest as nonspecific bindings, which are difficult, if not impossible, to titrate their site densities. Given these possible causes for the lifetime histograms to be multiexponential and the reverse rates and proportions of bonds of different types to be unknown, interpretation of such histograms can be difficult without additional experimental information provided by suitable controls.

QUANTAL BEHAVIOR

Perhaps the most appealing argument for seeing single bonds is the appearance of quantal behavior in the measurements of low number molecular interactions. This was initially observed in histograms of rupture (or unbinding) forces of biotin/avidin interactions measured with AFM, which exhibited multiple peaks that appeared periodic.¹⁷ This kind of histogram is exemplified in Fig. 4, which was obtained by the micropipette technique using human immunoglobulin G (IgG) coated RBC interacting with CD16a-expressing Chinese hamster ovary (CHO) cells. These experiments were done in a way similar to those described in Refs. 10 and 11. In addition to the detection of the presence of adhesion as was done in these previous reports, the micropipette aspirated RBC picoforce transducer was used to measure the force required to rupture the adhesions. The histogram of 1200 forces, measured from membrane elongation of the RBC that was retracted at a constant rate, peaks at bins of 18,

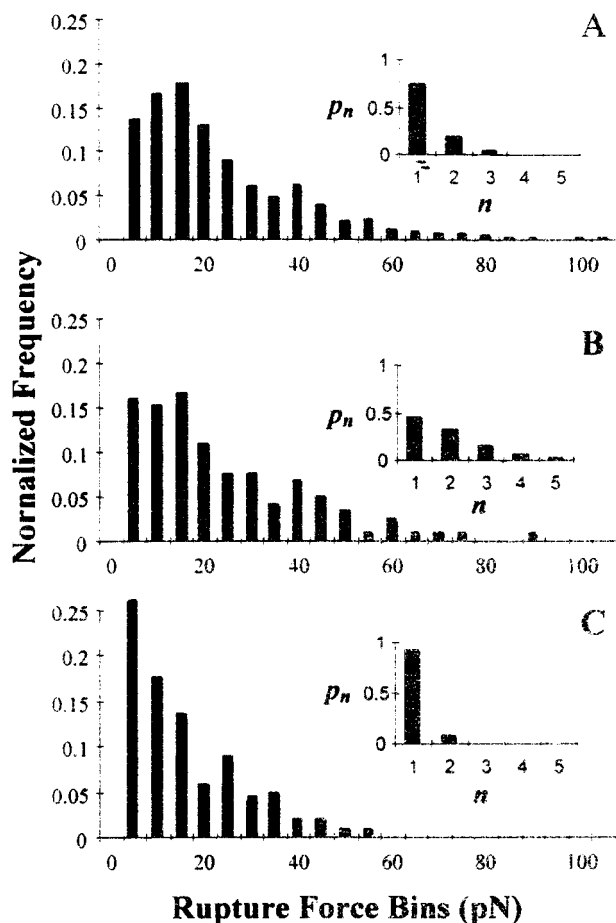


FIGURE 4. Detachment force histograms, measured by micropipette with constant rate ramping, of IgG-coated RBC from CD16a-expressing CHO cells, performed in a way similar to those described in Refs. 10 and 11. Insets: Probability distribution of bonds, p_n , that mediate the observed adhesions, predicted by the Poisson distribution from the measured adhesion probability, $P_{a|0}$, from the data in each panel. (A) All data, 1200 points at an average $P_{a|0}$ of 0.47. (B) Subpopulation of A, 100 points at an average $P_{a|0}$ of 0.76. (C) Subpopulation of A, 100 points at an average $P_{a|0}$ of 0.13.

40, and 55 pN, which appear to be integer multiples of a quantal unit 18 pN [Fig. 4(A)]. The frequencies of occurrence of these peak forces seem to correlate with the probabilities p_n of having 1, 2, and 3 bonds [Fig. 4(A), inset], calculated from the average $P_{a|0}$ ($=0.47$) using Poisson statistics. A subpopulation of these, 100 forces that were measured at a high $P_{a|0}$ ($=0.76$) value, resulted in a histogram with the same peak locations but altered relative heights [Fig. 4(B)]. These heights again correlate with p_n , which is now redistributed towards more likely having multiple bonds [Fig. 4(B), inset]. Another subpopulation of 100 forces that were measured at a low $P_{a|0}$ ($=0.13$) value resulted in a histogram with leftward shifted peak locations [Fig. 4(C)]. This is likely due to nonspecific binding, which comprises $\sim 7\%$ of total binding with much smaller rupture forces.

One interpretation of histograms such as those shown in Fig. 4 is based on a deterministic view: A single bond should have a defined strength below which it would remain intact and above which it would fail. n bonds would have an overall strength n times that of the single bond strength. Applying this view to analyze the rupture force histogram, the quantal unit was interpreted as the single-bond strength.¹⁷ However, such a deterministic view may not be valid at low loading rates.⁵³ Recently, more and more data support a probabilistic view: Non-covalent bonds dissociate stochastically, resulting in random rupture forces of a broad distribution, which is governed by the force dependence of reverse rate.^{4,13,15,30,53} Unless the loading rates are sufficiently high, there may be significant overlaps among distributions of forces required to rupture clusters of different number of bonds, which obscures their discrimination.⁵³

The term quantal behavior is generally used to describe measurements that appear to behave as superposition of a low number of “elementary quantities.” In essence, a quantal binding unit possesses invariant characteristics of measurements as they become less and less frequent, often resulted from the number of interactions involved being progressively decreased. Besides the rupture force case exemplified in Fig. 4, quantal behavior has also exhibited in other forms. The point attachments observed in the micropipette experiments behaved as quantal binding units because they appeared to form independently of each other and with equal probability, regardless of how much their frequency of occurrence decreased (Fig. 1). In the flow chamber experiment, while the frequency of cell tethering should decrease with decreasing site density, the distribution of the observed tether lifetimes should not change in the low site density regime where single molecular interaction is expected to be predominant. This kind of “quantal behavior” has indeed been observed, which has been used to argue that the observed tethering events are supported by single bonds.^{2,34}

However, although single bonds must behave as quantal binding units, quantal behavior does not necessitate single bonds. In other words, quantal behavior is a necessary but insufficient condition for single bonds. The reason is: There are several caveats that can critically affect data interpretation. The questions are: Does the quantal binding unit represent the elementary binding unit or the smallest detectable unit? Is the elementary binding unit a single bond or a cluster of bonds?

MULTIMERIC INTERACTION, CLUSTERING AND HETEROGENEOUS SURFACE

The existing criteria seem to be able to discriminate between a single bond and isolated multiple bonds that are spatially separated. It is the case of multibond clus-

ters or multimeric bonds that these criteria fail to work. This has been clearly demonstrated in a recent study comparing the dissociation kinetics of tethers between cells expressing either monomeric or dimeric forms of PSGL-1 and flow chamber floor coated with either monomeric or dimeric forms of P-selectin. Tethers supported by interactions between dimeric forms of P-selectin and PSGL-1 show an apparent k_r that increases much less rapidly with the applied force than those supported by interactions between monomeric forms of P-selectin and PSGL-1. Evidently, these data indicate that the former tethers contain more bonds (presumably dimeric bonds) than the latter tethers (presumably monomeric bonds). Tethers supported by interactions between dimeric P-selectin and monomeric PSGL-1 have an apparent k_r of intermediate force sensitivity, presumably because they contain a mixture of monomeric and dimeric bonds.³⁷

It should be emphasized that other than the difference in their apparent reverse rates equal lines of supporting evidence appear to exist for them to be single-bond tethers, namely, tethers in all cases were discrete and infrequent and appeared to follow first-order irreversible dissociation kinetics, which appeared to be independent of the P-selectin density when it was low. Moreover, preliminary AFM measurements indicate that although the rupture force histograms of dimeric PSGL-1 were rightward shifted towards larger forces compared to those of monomeric PSGL-1, dimeric PSGL-1 histograms exhibited a single peak rather than two peaks of integer multiples of the peak force of the single-peaked monomeric PSGL-1 histograms, contrary to what is predicted from the deterministic theory of single-bond strength (B. Marshall, M. Long, R. McEver, and C. Zhu, unpublished data). A lesson learned from this example is that it is important to use monomeric molecules in the experimental preparation. It also calls for reevaluation of published results obtained using dimeric molecules, e.g., those created by replacing the Fab fragments of IgG with the molecule of interest to make it soluble, in studies attempting to measure single-bond interactions.

Clustering may be an evolved strategy to achieve greater effectiveness and/or higher strengthening of adhesion required by many biological functions other than uniform molecular distribution.^{5,45,47,52} In addition to multimeric interactions, other clustering mechanisms include microvilli with concentrated adhesion molecules, such as L-selectin²⁰ and PSGL-1,⁶ at the tips and membrane rafts with concentrated glycosyl phosphatidylinositol-anchored proteins in glycosphingolipid and cholesterol-enriched microdomains.³ Clustering renders high local densities of receptors and/or ligands that may not be lowered by decreasing the global or average densities, thereby likely resulting in multiple bonds, which prevent us from applying the existing cri-

teria for single bonds. Clustering also creates surface heterogeneity, which, like the previously discussed multispecies binding, may obscure data interpretation. Another form of surface heterogeneity is surface roughness, such as microvillous, which is prevalent in nucleated cells. The much larger dimensions of surface roughness compared to those of the molecules may lead to their selective presentation. Differences in the accessibility of different subpopulations of molecules may complicate interpretation based on average measurements.

RUPTURE FORCE AND EXPECTED SINGLE-BOND STRENGTH

In an earlier example, it was the comparison between the characteristics of monomeric and dimeric P-selectin/PSGL-1 interactions that demonstrated that the latter could not have been single bonds. This suggests that the most reliable criteria for determining single bonds may be that the measured quantities match the known features of single bonds. Unfortunately, our journey begins from where single-bond properties are not known. So, one is forced to use a less rigorous criterion of requiring that the measured quantities match the “expected” or “predicted” features of single bonds. Perhaps the most commonly used test in this regard is comparing the measured rupture forces with the order-of-magnitude range of antigen/antibody bond strength of 10–100 pN very crudely estimated using a purely theoretical analysis by Bell.⁴ More recently, molecular dynamics simulations were used to calculate the force required to rupture an avidin/biotin bond within the nanosecond range, which estimates strengths of several hundreds of piconewtons.^{18,21} Thus, the forces required to rupture the CD16a/hIgG-mediated point attachments are seen from Fig. 4 to be of the order of several tens of piconewtons, with a quantized “strength” of ~ 18 pN. This would then be deemed as consistent with the predicted strength of single bonds; and it would in turn be used to argue that the point attachments are supported by single bonds. Obviously, evidence like this is circumstantial at best.

EFFECTS OF SENSITIVITY CUTOFF

All adhesion sensors have a sensitivity cutoff; the smallest binding unit a sensor could detect may appear infrequently but may still be composed of multiple bonds. Thus, a critical requirement for single-bond measurements is to use an adhesion sensor sufficiently sensitive such that not even interactions as weak and as short lived as those mediated by a single bond would go undetected. The question is, how can one be certain that this is the case?

The sensitivity of an adhesion detector includes two aspects: the smallest detectable force and the minimum

time required for detection. The rupture force and lifetime of a bond are believed to be broadly distributed random variables.⁵³ Moreover, there are extensive overlaps among the rupture force/lifetime of adhesions mediated by a single, double, triple, ..., bonds (Fig. 4). Therefore, as the adhesion detector gradually loses its sensitivity, it would miss more and more weak and short-lived adhesion events. This line of reasoning suggests a simple test for the adequacy of the adhesion detector: to check the dependence of the occurrence frequency of the detectable events on the sensitivity threshold. The lack of changes in the adhesion probability with the changing sensitivity cutoff after it has been tuned sufficiently low is considered as evidence that most single bonds could not have gone undetected.⁵¹

The above approach is analogous to the filtering method employed by electrophysiologists in single-channel analysis where the lack of change in the current histogram when signals are filtered at different frequencies is considered as indicative that a single channel is recorded. The same technique can be applied to lifetime analysis with the flow chamber. Here, limited time resolution may lead to missing the fast dissociating component, yielding a straight line in an otherwise two-segment $\ln(P_a)$ vs t curve. The resulting straight line may represent the steady-state detachment of multibond tethers or the slowly dissociating component of a dual-step or dual-species binding (Fig. 3).³³ Indeed, using a high-speed camera to collect data, Smith *et al.* have revealed faster off rates of selectin/ligand binding than those estimated from data obtained using standard video rate cameras, suggesting previous measurements were not single-bond events.⁴⁰

Similar to comparing parameters evaluated from data collected with different detector sensitivities, another strategy is to compare the same parameter evaluated by different methods. For example, for a single-exponential distribution characteristic of the first-order irreversible dissociation kinetics, k_r can be estimated from either the negative slope of the $\ln(P_{a1})$ vs t line, the reciprocal average, $1/\langle t \rangle$, or reciprocal standard deviation, $1/\sigma(t)$, of lifetimes. Comparison among these three estimates would thus provide a test for the single-bond hypothesis. Similar tests can be performed using the presumed single-bond strength derived from the force histogram that exhibits the quantal force characteristic, discussed earlier, or from the relationship between the mean and variance of random forces that follow a Poisson distribution.⁴⁸

CONCLUDING REMARKS

We have examined the supporting evidence and caveats for single-bond measurements. Existing criteria appear able to discriminate between single and multiple

bonds if the latter are spatially isolated (hence, can be diluted) and of a simple kinetic mechanism (e.g., first-order irreversible dissociation). The remaining difficulties are mainly concerned with complex binding schemes, multimeric interactions, clustering, and heterogeneous surfaces. These have to be addressed with proper experimental design and careful controls. It seems reasonable to conclude that no single criterion is sufficient for a formal proof that single-binding events are actually observed. However, the cumulative body of evidence may provide reasonable confidence.

ACKNOWLEDGMENTS

The authors thank Rodger P. McEver for the generous gifts of the P-selectin reagents. This work was supported by NIH Grant Nos. AI38282 and AI44902 (C.Z.) as well as by NSFC Grant Nos. 10042001 and 10072071, a CAS Hundreder Project Award and a TRAPOYT Award of China (M.L.). One of the authors (M.L.) is a recipient of senior scholarship from Ministry of Education of China. One of the authors (S.C.) was partially supported by NIH training Grant No. GM08433.

REFERENCES

- ¹Alon, R., S. Chen, K. D. Puri, E. B. Finger, and T. A. Springer. The kinetics of L-selectin tethers and the mechanics of selectin-mediated rolling. *J. Cell Biol.* 138:1169–1180, 1997.
- ²Alon, R., D. A. Hammer, and T. A. Springer. Lifetime of the P-selectin–carbohydrate bond and its response to tensile force in hydrodynamic flow. *Nature (London)* 374:539–542, 1995.
- ³Anderson, R. G. The caveolae membrane system. *Annu. Rev. Biochem.* 67:199–225, 1998.
- ⁴Bell, G. I. Models for the specific adhesion of cells to cells. *Science* 200:618–627, 1978.
- ⁵Berlin, C., R. F. Bargatze, J. Campbell, U. H. von Andrian, C. Szabo, S. R. Hasslen, R. D. Nelson, E. L. Berg, S. L. Erlandsen, and E. C. Butcher. $\alpha 4$ integrins mediate lymphocyte attachment and rolling under physiological flow. *Cell* 80:413–422, 1995.
- ⁶Bruehl, R. E., K. I. Moore, D. E. Lorant, N. Borregaard, G. A. Zimmerman, R. P. McEver, and D. F. Bainton. Leukocyte activation induces surface redistribution of P-selectin glycoprotein ligand-1. *J. Leukoc. Biol.* 61:489–499, 1997.
- ⁷Chang, K.-C., D. F. J. Tees, and D. A. Hammer. The state diagram for cell adhesion under flow: Leukocyte rolling and firm adhesion. *Proc. Natl. Acad. Sci. U.S.A.* 97:11262–11267, 2000.
- ⁸Chen, S., and T. A. Springer. An automatic braking system that stabilizes leukocyte rolling by an increase in selectin bond number with shear. *J. Cell Biol.* 94:185–200, 1999.
- ⁹Chen, S., and T. A. Springer. Selectin receptor–ligand bonds: Formation limited by shear rate and dissociation governed by the Bell model. *Proc. Natl. Acad. Sci. U.S.A.* 98:950–955, 2001.
- ¹⁰Chesla, S. E., P. Li, S. Nagarajan, P. Selvaraj, and C. Zhu. The membrane anchor influences ligand binding two-dimensional kinetic rates and three-dimensional affinity of Fc γ RIII (CD16). *J. Biol. Chem.* 275:10235–10246, 2000.
- ¹¹Chesla, S. E., P. Selvaraj, and C. Zhu. Measuring two-dimensional receptor–ligand binding kinetics with micropipette. *Biophys. J.* 75:1553–1572, 1998.
- ¹²Cozens-Roberts, C., D. A. Lauffenburger, and J. A. Quinn. Receptor-mediated cell attachment and detachment kinetics. I. Probabilistic model and analysis. *Biophys. J.* 58:841–856, 1990.
- ¹³Evans, E. Probing the relation between force, lifetime, and chemistry in single molecular bonds. *Annu. Rev. Biophys. Biomol. Struct.* 30:105–128, 2001.
- ¹⁴Evans, E., D. Berk, and A. Leung. Detachment of agglutinin-bonded red blood cells. I. Forces to rupture molecular-point attachments. *Biophys. J.* 59:838–848, 1991.
- ¹⁵Evans, E., and K. Ritchie. Dynamic strength of molecular adhesion bonds. *Biophys. J.* 72:1541–1555, 1997.
- ¹⁶Evans, E., K. Ritchie, and R. Merkel. Sensitive force technique to probe molecular adhesion and structural linkages at biological interfaces. *Biophys. J.* 68:2580–2587, 1995.
- ¹⁷Florin, E. L., V. T. Moy, and H. E. Gaub. Adhesion forces between individual ligand–receptor pairs. *Science* 264:415–417, 1994.
- ¹⁸Grubmüller, H., B. Heymann, and P. Tavan. Ligand binding: Molecular mechanics calculation of the streptavidin–biotin rupture forces. *Science* 271:997–999, 1996.
- ¹⁹Hammer, D. A., and S. M. Apte. Simulation of cell rolling and adhesion on surfaces in shear flow: General results and analysis of selectin-mediated neutrophil adhesion. *Biophys. J.* 63:35–57, 1992.
- ²⁰Hasslen, S. R., A. R. Burns, S. I. Simon, C. W. Smith, K. Starr, A. N. Barclay, S. A. Michie, R. D. Nelson, and S. L. Erlandsen. Preservation of spatial organization and antigenicity of leukocyte surface molecules by aldehyde fixation: Flow cytometry and high-resolution FESEM studies of CD62L, CD11b, and Thy-1. *J. Histochem. Cytochem.* 44:1115–1122, 1996.
- ²¹Izrailev, S., S. Stepaniants, M. Balsera, Y. Oono, and K. Schulten. Molecular dynamics study of unbinding of the avidin–biotin complex. *Biophys. J.* 72:1568–1581, 1997.
- ²²Kaplanski, G., C. Farnarier, O. Tissot, A. Pierres, A.-M. Benoliel, M.-C. Alessi, S. Kaplanski, and P. Bongrad. Granulocyte-endothelium initial adhesion. Analysis of transient binding events mediated by E-selectin in a laminar shear flow. *Biophys. J.* 64:1922–1933, 1993.
- ²³King, M. R., and D. A. Hammer. Multiparticle adhesive dynamics. Interactions between stably rolling cells. *Biophys. J.* 81:799–813, 2001.
- ²⁴Kuo, S. C., D. A. Hammer, and D. A. Lauffenburger. Simulation of detachment of specifically bound particles from surfaces by shear flow. *Biophys. J.* 73:517–531, 1997.
- ²⁵Laurenzi, I. J., and S. L. Diamond. Monte Carlo simulation of the heterotypic aggregation kinetics of platelets and neutrophils. *Biophys. J.* 77:1733–1746, 1999.
- ²⁶Lee, G. U., D. A. Kidwell, and R. J. Colton. Sensing discrete streptavidin–biotin interactions with atomic force microscopy. *Langmuir* 10:354–357, 1994.
- ²⁷Long, M., H. L. Goldsmith, D. F. Tees, and C. Zhu. Probabilistic modeling of shear-induced formation and breakage of doublets cross-linked by receptor–ligand bonds. *Biophys. J.* 76:1112–1128, 1999.
- ²⁸Long, M., H. Zhao, K.-S. Huang, and C. Zhu. Kinetic measurements of cell surface E-selectin/carbohydrate ligand interactions. *Ann. Biomed. Eng.* 29:935–946, 2001.

- ²⁹McQuarrie, D. A. Kinetics of small systems I. *J. Chem. Phys.* 38:433–436, 1963.
- ³⁰Merkel, R., P. Nassoy, A. Leung, K. Ritchie, and E. Evans. Energy landscapes of receptor–ligand bonds explored with dynamic force spectroscopy. *Nature (London)* 397:50–53, 1999.
- ³¹Miyata, H., R. Yasuda, and K. Kinoshita. Strength and lifetime of bonds between actin and skeletal muscle alpha-actinin studied with an optical trapping technique. *Biochim. Biophys. Acta* 1290:83–88, 1996.
- ³²Pierres, A., A. M. Benoliel, and P. Bongrand. Measuring the lifetime of bonds made between surface-linked molecules. *J. Biol. Chem.* 270:26586–26592, 1995.
- ³³Pierres, A., A.-M. Benoliel, and P. Bongrand. Initial steps of cell–substrate adhesion. In: *Cell Mechanics and Cellular Engineering*, edited by V. C. Mow, F. Guilak, R. Tran-Son-Tay, and R. M. Hochmuth. New York: Springer, 1994, pp. 145–159.
- ³⁴Pierres, A., O. Tissot, and P. Bongrand. Analysis of the motion of cells driven along an adhesive surface by a laminar shear flow. In: *Studying Cell Adhesion*, edited by P. Bongrand, P. Claesson, and A. Curtis. Heidelberg: Springer, 1994, pp. 157–174.
- ³⁵Piper, J. W., R. A. Swerlick, and C. Zhu. Determining force dependence of two-dimensional receptor–ligand binding affinity by centrifugation. *Biophys. J.* 74:492–513, 1998.
- ³⁶Ramachandran, V., M. U. Nollert, H. Qiu, W. J. Liu, R. D. Cummings, C. Zhu, and R. P. McEver. Tyrosine replacement in P-selectin glycoprotein ligand-1 affects distinct kinetic and mechanical properties of bonds with P- and L-selectin. *Proc. Natl. Acad. Sci. U.S.A.* 96:13771–13776, 1999.
- ³⁷Ramachandran, V., T. Yago, T. K. Epperson, M. Kobzdej, M. U. Nollert, R. D. Cummings, C. Zhu, and R. P. McEver. Dimerization of a selectin and its ligand stabilizes cell rolling and enhances tether strength in shear flow. *Proc. Natl. Acad. Sci. U.S.A.* 98:10166–10171, 2001.
- ³⁸Shao, J. Y., and R. M. Hochmuth. Micropipette suction for measuring pico-Newton forces of adhesion and tether formation from neutrophil membranes. *Biophys. J.* 71:2892–2901, 1996.
- ³⁹Shao, J. Y., and R. M. Hochmuth. Mechanical anchoring strength of L-selectin, beta2 integrins, and CD45 to neutrophil cytoskeleton and membrane. *Biophys. J.* 77:587–596, 1999.
- ⁴⁰Smith, M. J., E. L. Berg, and M. B. Lawrence. A direct comparison of selectin-mediated transient, adhesive events using high temporal resolution. *Biophys. J.* 77:3371–3383, 1999.
- ⁴¹Tees, D. F., O. Coenen, and H. L. Goldsmith. Interaction forces between red cells agglutinated by antibody. IV. Time and force dependence of breakup. *Biophys. J.* 65:1318–1334, 1993.
- ⁴²Tees, D. F. J., R. E. Waugh, and D. A. Hammer. A micro-cantilever device to assess the effect of force on the lifetime of selectin–carbohydrate bonds. *Biophys. J.* 80:668–682, 2001.
- ⁴³Tha, S. P., J. Shuster, and H. L. Goldsmith. Interaction forces between red cells agglutinated by antibody. II. Measurement of hydrodynamic force of breakup. *Biophys. J.* 50:1117–1126, 1986.
- ⁴⁴Thoumine, O., P. Kocian, A. Kottelat, and J. J. Meister. Short-term binding of fibroblasts to fibronectin: Optical tweezers experiments and probabilistic analysis. *Eur. Biophys. J.* 29:398–408, 2000.
- ⁴⁵van Kooyk, Y., P. Weder, K. Heije, and C. G. Figdor. Extracellular calcium modulates leukocyte function-associated antigen-1 cell surface distribution on T lymphocytes and consequently affects cell adhesion. *J. Cell Biol.* 124:1061–1070, 1994.
- ⁴⁶Vijayendran, R., D. Hammer, and D. Leckband. Simulations of the adhesion between molecularly bonded surfaces in direct force measurements. *J. Chem. Phys.* 108:7783–7793, 1998.
- ⁴⁷von Andrian, U. H., S. R. Hasslen, R. D. Nelson, S. L. Erlandsen, and E. C. Butcher. A central role for microvillous receptor presentation in leukocyte adhesion under flow. *Cell* 82:989–999, 1995.
- ⁴⁸Williams, J. M., T. Han, and T. P. J. Beebe. Determination of single-bond forces from contact force variances in atomic force microscopy. *Langmuir* 12:1291–1295, 1996.
- ⁴⁹Williams, T. E., S. Nagarajan, P. Selvaraj, and C. Zhu. Concurrent binding to multiple receptors: Kinetic rates of CD 16b and CD32a for IgG. *Biophys. J.* 79:1867–1875, 2000.
- ⁵⁰Williams, T. E., S. Nagarajan, P. Selvaraj, and C. Zhu. Quantifying the impact of membrane microtopology on effective two-dimensional affinity. *J. Biol. Chem.* 276:13283–13288, 2001.
- ⁵¹Williams, T. E., and C. Zhu. Concurrent binding to multiple ligands: Kinetic rates of CD16b for membrane-bound IgG1 and IgG2. *Biophys. J.* 79:1858–1866, 2000.
- ⁵²Yap, A. S., W. M. Briehner, M. Priushy, and B. M. Gumbiner. Lateral clustering of the adhesive ectodomain: A fundamental determinant of cadherin function. *Curr. Biol.* 7:308–315, 1997.
- ⁵³Zhu, C., G. Bao, and N. Wang. Cell mechanics: Mechanical response, cell adhesion, and molecular deformation. *Annu. Rev. Biomed. Eng.* 2:189–226, 2000.